A Probable z∼7 Galaxy Strongly Lensed by the Rich Cluster Abell 2218: Exploring the Dark Ages

Jean-Paul Kneib[1,2], Richard S. Ellis[2], Michael R. Santos [2,3] Johan Richard[1,2]

ABSTRACT

We discuss the observational properties of a remarkably faint triply-imaged galaxy revealed in a deep z'-band Advanced Camera for Surveys observation of the lensing cluster Abell 2218 (z =0.175). A well-constrained mass model for the cluster, which incorporates the outcome of recent Keck spectroscopic campaigns, suggests that the triple system arises via a high redshift ($z > 6$) source viewed at high magnification ($\simeq \times 25$). Optical and infrared photometry from Hubble Space Telescope and the Keck Observatory confirms the lensing hypothesis and suggests a significant discontinuity occurs in the spectral energy distribution within the wavelength interval 9250–9850Å. If this break is associated with Gunn-Peterson absorption from neutral hydrogen, a redshift of $6.6 < z < 7.1$ is inferred. Deep Keck spectroscopy conducted using both optical and infrared spectrographs fails to reveal any prominent emission lines in this region. However, an infrared stellar continuum is detected whose decline below 9800Å suggests a spectroscopic redshift towards the upper end of the range constrained photometrically, i.e. $z \simeq 7$. Regardless of the precise redshift, the source is remarkably compact ($\lesssim 1\, h_{70}^{-1}$kpc) and faint (z_{F850LP} =28.0) yet is undergoing vigorous star formation at a rate $\simeq 2.6\ M_{\odot}\mathrm{yr}^{-1}$. An intriguing property is the steep slope of the ultraviolet continuum implied by the photometry which may suggest that the source is representative of an early population of galaxies responsible for cosmic reionization. Independent verification of these results is highly desirable but our attempts highlight the difficulty of studying such sources with present facilities and the challenges faced in pushing back the frontiers of the observable universe beyond $z \sim 6.5$.

[0]Using data obtained with the Hubble Space Telescope operated by AURA for NASA and the W.M. Keck Observatory on Mauna Kea, Hawaii. The W.M. Keck Observatory is operated as a scientific partnership among the California Institute of Technology, the University of California and NASA and was made possible by the generous financial support of the W.M. Keck Foundation.

[1]Observatoire Midi-Pyrénées, UMR5572, 14 Avenue Edouard Belin, 31000 Toulouse, France

[2]Caltech, Astronomy, 105-24, Pasadena, CA 91125, USA

[3]Institute of Astronomy, Madingley Road, Cambridge, CB3 0HA, UK

Subject headings: cosmology: observations, galaxies: formation, galaxies: evolution, gravitational lensing

1. Introduction

Reionization was a landmark event which imprinted a signature over the scale of the entire universe. After decades of lower limits on the redshift at which it occurred, recent observations of QSOs discovered by the Sloan Digital Sky Survey (Becker et al. 2001; Djorgovski et al. 2001, Fan et al. 2002) suggest that reionization was just finishing at $z \sim 6-6.5$. The discovery of $z \simeq 6.5$ galaxies with strong Lyman α emission (Hu et al. 2002, Kodaira et al. 2003) is illustrative of possible sources which may be responsible. Analysis of recent temperature and polarization fluctuation data from the *WMAP* satellite suggests an optical depth for Thompson scattering of $\tau = 0.17 \pm 0.04$, implying that reionization began at higher redshift, perhaps as early as $z \sim 15 - 20$ (Kogut et al. 2003, Spergel et al. 2003).

The discovery of star-forming galaxies at $z \simeq 6.5$ is an important step toward understanding the nature of the sources responsible for the end of cosmic reionization. However, to explore the earlier stages implied by the *WMAP* results, it is necessary to push the search for star forming systems to higher redshifts. With current facilities this is technically very challenging. It is perhaps salutary to note that the current redshift frontier ($z = 6.5$, corresponding to an observed Lyman α wavelength of 9200Å) is coincident with the wavelength at which optical CCD detectors fall significantly in their quantum efficiency. Ground-based infrared spectroscopy, necessary for exploring sources at higher redshift, is especially difficult at faint limits.

Color-based searches for $z >$6 sources with the Advanced Camera for Surveys (*ACS*) on-board the Hubble Space Telescope (*HST*) is now recognized as a valuable way of locating $z > 6$ sources. Promising results have been obtained by utilizing the long wavelength F850LP (z'-band) filter in conjunction with deep infrared imaging on *HST* or with large ground-based telescopes (Bouwens et al. 2003, Yan et al. 2003, Stanway et al. 2003, Dickinson et al. 2003). In view of significant contamination of red 'drop-out' samples by cool stars (e.g. Stanway et al. 2003), the primary challenge lies in spectroscopically verifying faint candidates (e.g. Dickinson et al. 2000). Neither optical nor infrared spectrographs on the current generation of ground-based telescopes may have the sensitivity to give convincing results unless strong emission lines are present. Although most of the distant sources found beyond $z \simeq$5 have been identified via strong Lyman α emission (Stern & Spinrad 1999, Spinrad 2003), some sources should have weak or no Lyman α emission (e.g. Spinrad et al. 1998). Indeed, a significant fraction ($\sim$ 75%) of the most intensely star-forming galaxies located by color

selection techniques at $z \simeq 3$, reveal Lyman α only in absorption (Shapley et al. 2003).

Gravitational magnification by foreground clusters of galaxies, whose mass distributions are tightly constrained by arcs and multiple images of known redshift, has already provided new information on the abundance of high redshift objects (Kneib et al 1996, Santos et al. 2003). Particularly high magnifications ($\simeq \times$10-50) are expected in the *critical regions* which can be located precisely in well-understood clusters for sources occupying specific redshift ranges (Ellis et al. 2001). Although the volumes probed in this way are far smaller than those addressed in panoramic narrow band surveys (Hu et al. 1998, Malhotra et al. 2001, Hu et al. 2003) or the color-based surveys cited earlier, if the surface density of background sources is sufficient, lensing may provide the necessary boost for securing the first glimpse of young cosmic sources beyond $z \simeq$6.5 (Santos et al. 2003).

In the course of studying the detailed rest-frame properties of the image pair of a lensed $z = 5.576$ galaxy in the cluster Abell 2218 (Ellis et al 2001), we have discovered a new faint pair of images in a deep z'-band *ACS* observation of this cluster. Based on the geometrical configuration of this pair and its photometric properties, we concluded that the images most likely arise via strong magnification of a distant $z >$6 source. The implied high redshift of this source led us to explore its properties in more detail.

A plan of the paper follows. We present the photometric observations in Section 2. Section 3 discusses redshift constraints determined independently from the lensing model of Abell 2218 and the spectral energy distribution based on broad-band photometry. Section 4 summarizes our attempts to detect Lyman α emission spectroscopically and discusses the implications of a continuum discontinuity seen in the infrared spectrum. We discuss the source properties and implications further in Section 5. Throughout we assume a cosmological model with $\Omega_{\rm M} = 0.3$, $\Omega_\Lambda = 0.7$ and $\rm H_0$=70 km s^{-1} Mpc^{-1}.

2. Photometric Observations

The source in question was originally discovered as a pair of images (*a* and *b* on Figure 1) with reflection symmetry and a separation of 7″ in a deep (5-orbit, 11.31 ksec) *HST*/*ACS*-F850LP (z'-band) observation of the Abell 2218 cluster of galaxies. The observation was conducted as part of GO program 9452 (PI: Ellis) to characterize the stellar continuum in the lensed pair at z=5.576 discussed earlier by Ellis et al. (2001).

The new *ACS* images were reduced using standard IRAF[4] and STSDAS routines. The

[4]IRAF is distributed by the National Optical Astronomy Observatories, which are operated by the

source was found by blinking the reduced F850LP image with two archival images taken at shorter wavelength with the F814W and F606W filters of the Wide Field Planetary Camera 2 (*WFPC2*) (SM-3a ERO program 8500, PI: Fruchter; exposure time F606W: 10 ksec, F814W: 12 ksec). A prominent discontinuity in the brightness of the pair can be seen viewing, in sequence, the F850LP, F814W and F606W frames (Figure 1). Together with the geometrical arrangement and symmetry of the pair in the context of our mass model for Abell 2218, this suggested the source is at high redshift and gravitationally magnified by the cluster (see §3).

The two images have similar appearance in the *HST*/NICMOS F160W image. This H-band data was also obtained under the GO program 9452 and was acquired in a 4-orbit CVZ observation totalizing 22.2 ksec of exposure time. Similarly, we also identified the lensed pair in a deep Keck NIRC J-band image (5.64 ksec exposure) taken in 0.65″seeing on July 22 and 23, 2002 (Blain and Reddy private communication).

A clear mirror symmetry is seen in the *HST* data; both images contain a bright core, a second fainter knot and extended emission of lower surface brightness. The orientation of the pair also closely matches the predicted shear direction (Figure 1). The lensing hypothesis is further verified by comparing the colors of the two images a and b using the available photometric data summarized in Table 1[5]. Colors were computed using a fixed elliptical aperture, and are identical for both images within the uncertainties. (For the $z_{850LP} - J$ color, the *ACS* z'-band image was convolved by a gaussian to match the seeing of the Keck NIRC J image).

Association of Universities for Research in Astronomy, Inc., under cooperative agreement with the National Science Foundation.

[5]All photometric quantities are based on the Vega system

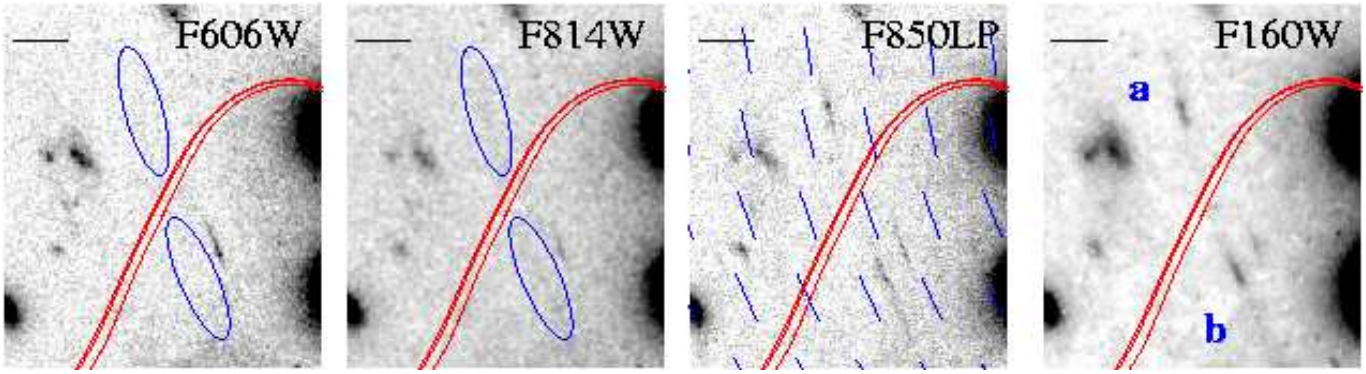

Figure 1: *WFPC2*-F606W, *WFPC2*-F814W, *ACS*-F850LP and NICMOS-F160W images of Abell 2218 of the new faint pair in the lensing cluster Abell 2218 (z=0.175). The signals redward of the *WFPC2*-F814W observation suggests a marked break occurs in the continuum signal at around 9600Å . Red lines correspond to the predicted location of the critical lines at z_s=5,6.5 and 7 (from bottom to top, the latter two being almost coincident). The scale bar at the top left of each image represents 2″. The predicted shear direction (thin blue lines) closely matches the orientation of the lensed images.

see jpeg file

Figure 2: (Top) Location of the image pair a, b and the third image c in a pseudo-color image made from the *WFPC2*-F606W, F814W and *ACS*-F850LP images. The red curves refers to the critical lines of infinite magnification for sources placed at z=5.576 and z=7.0 in the context of Kneib et al's (1996) mass model revised to include the z=5.576 pair (shown as unlabelled circles at the top of the figure) discussed by Ellis et al. (2001) and a triply-imaged SCUBA source at z=2.515 (Kneib et al. 2004a). (Bottom) Pseudo-color representation of the three images demonstrating their association with a single lensed source.

3. Redshift Constraints

3.1. Gravitational Lensing

In the context of the tightly-constrained mass model of Abell 2218 (Kneib et al. 1996), updated to include the properties of the z=5.576 pair identified by Ellis et al. (2001) and the more recent confirmation of a triply-imaged sub-millimeter selected source at z=2.515 (Kneib et al. 2004a), the symmetry expected for a lensed pair around the critical line implies a source redshift z_s >6 (see curves in Figure 1). The absolute location of the z=6 critical line is particularly well understood in this region from the measured symmetry of the adjacent z=5.576 pair around its critical line shown in Figure 2. However, the lensing configuration for the new source provides only a fairly weak constraint on the precise redshift beyond this lower limit since the location of the critical line does not change significantly beyond $z \simeq 6$ (Figure 1).

Our mass model for Abell 2218 requires there to be a third image of the source, which we successfully located in the z'-band image at the expected position (image c in Figure 2) and with the expected flux (Table 1). Although our photometric coverage of this third, fainter, image is not as complete as that for the primary pair (because of the smaller field of the infrared cameras used), importantly the *HST* photometry confirms the same discontinuity in flux seen between F850LP and F606W (Figure 2, Table 1). The improved mass model suggests that all 3 images represent manifestations of a single source at z >6 magnified by a factor of $\simeq$25 (in the case of images a and b). The intrinsic (unlensed) source brightness is $z_{850LP} = 28.0 \pm 0.1$, $H_{160W} = 26.5 \pm 0.1$.

3.2. Spectral Energy distribution

Figure 3 summarizes the available broad-band photometry for the brightest of the three images (a in Figure 1). We include, for completeness, the Keck NIRC J measurement although, as a ground-based measurement it is more adversely affected by crowding and background issues related to the adjacent luminous cluster members. Its low significance provides little more than evidence for a detection. Accordingly, we do not use the J band data in any of the subsequent analysis.

A significant discontinuity in flux is apparent in the wavelength interval $\lambda\lambda$ ~9200Å–1μm. The overlap in sensitivity between the WFPC-2 filter F814W and the *ACS* filter F850LP is of particular diagnostic use. If it is assumed the $z > 6$ source has a UV continuum which rises to shorter wavelengths with a discontinuity produced by a Gunn-Peterson trough

at around λ_{rest}=1216Å, the ratio of the F814W and F850LP fluxes can be used to estimate the redshift depending on the slope of the UV continuum.

Assuming the spectral energy distribution is given by a simple relation: $f(\lambda) \propto \lambda^{-\alpha}$ for $\lambda/(1+z)$ >1216Å and $f(\lambda) = 0$ otherwise, the accurate *HST* photometry (F606W, F814W, F850LP, F160W) implies the discontinuity occurs in the wavelength interval 9250–9850Å, corresponding to 6.6< z <7.1 (see dashed lines in Figure 3)[6]. The photometric redshift constraint is particularly firm at the lower end. Below $z \simeq$6.6 it is hard to justify the observed F814W and F850LP flux ratio regardless of the form of the spectral energy distribution. In summary, therefore, the available HST photometry suggests the lensed source lies beyond $z \simeq$6.6.

4. Optical and Infrared Spectroscopy

Given the possibility that the lensed source lies beyond a redshift $z \simeq$6.6 with a Gunn-Peterson discontinuity in the wavelength range 9250–9850Å we next tried to detect Lyman α emission in this region using both the Near Infrared Spectrograph (NIRSPEC, McLean et al. 2001) on Keck II and the Low Resolution Imaging Spectrograph (LRIS, Oke et al. 1998) on Keck I. If around half of the flux in the F850LP band arises via a Lyman α emission line, in a manner analogous to the z =5.576 source (Ellis et al. 2001), we considered that the LRIS campaign should be successful in securing the redshift, particularly since the lower part of the region to explore is, by good fortune, one of the "windows" of low OH sky emission used by narrow band imagers to locate Lyman α emitters (e.g. Kodaira et al. 2003).

We used LRIS on two runs, May 31 - June 1 2003 and June 30 - July 1 2003 (see Kneib et al. 2004b for a complete description of these data). During the first observing run we observed the brighter pair of the triple system using the 600 line grating blazed at 1μm for a total of 13.8 ksec. The first night offered relatively poor conditions (cirrus, high humidity) but 9.0 ksec was secured on the second night in slightly better conditions. For these observations the wavelength coverage ranged from 6930 to 9500Å. No signal was detected from either image.

During the second observing run, we used the same configuration and integrated for 9.2 ksec in relatively good conditions with $\sim 0.8''$ seeing. The wavelength coverage was extended slightly to the red to reach 9600Å. In the following, only the second observing run

[6]Although the weak NIRC J detection suggests a shallower UV slope, we give this discrepancy low weight in view of the superior quality of the HST data

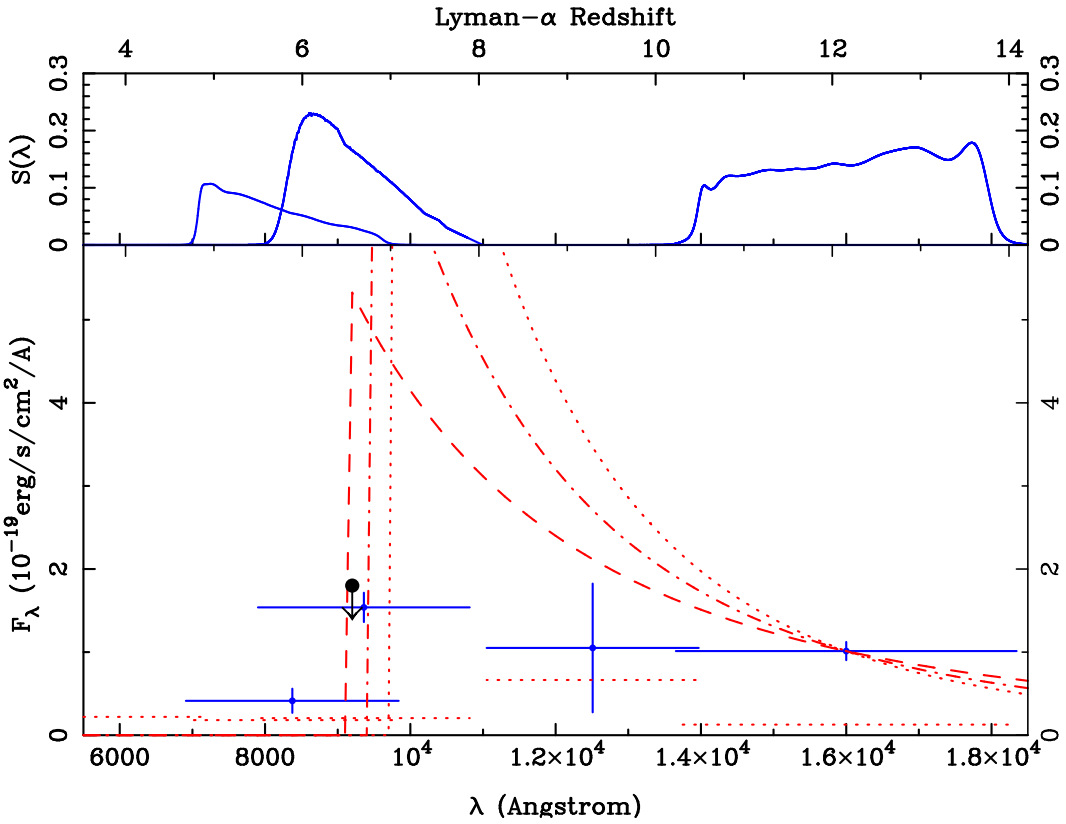

Figure 3: (Top) Relative efficiencies of the filter+instrument used in our photometric observations. From left to right: *WFPC2*-F814W, *ACS*-F850LP and *NICMOS*-F160W. (Bottom) Spectral energy distribution of image *a* uncorrected for lensing magnification. Photometric points are indicated by blue crosses, and the 3σ point source detection limits are indicated by a horizontal dashed red lines below each data point. The non-detection of the continuum in the LRIS 9000–9300Å window is indicated by the black arrow. Red dashed lines correspond to power law spectral energy distributions (with $f \propto \lambda^{-\alpha}$ for $\lambda/(1+z) > 1216$Å and $f = 0$ otherwise) with slope indices (from bottom to top at 1.2 10^4 Å) of α=3,4 and 5. The available data are consistent with a neutral hydrogen break in the interval 9250–9850Å corresponding to $6.6 < z < 7.1$.

will be utilized as the data quality is much better. Flux calibration was conducted using Feige 67, Feige 110 and Wolf 1346 spectrophotometric standards observed in twilight. The spectroscopic observations were reduced using IRAF. Despite the improved conditions, no continuum or emission lines were detected to 9600Å from either image. The absence of any LRIS detection in the clean wavelength range 9000-9300 Å places an additional constraint on the lower redshift limit. In Figure 3 we illustrate this via an upper limit on the absolute flux (black symbol) which further suggests the source lies beyond $z \simeq 6.6$.

The NIRSPEC (McLean et al. 1998) observations were obtained with the Keck II telescope on the nights of May 10 and 11 2003. The spectrograph was used in low-dispersion mode using a filter with transmission from 9500 to 11200Å. A slit width of $0.76''$ was used to acquire the pair giving a spectral resolution of R=1100. We obtained 37 exposures of 900 sec yielding a total integration time of 33 ksec. We dithered along the slit between two different positions, verifying our pointing on a nearby reference star using the slit-viewing guide camera at each dither. These observations were also reduced using IRAF. Individual spectra were registered using offsets determined from simultaneous images obtained with the slit-viewing guide-camera. Our optimally combined spectrum of each image comprised 26 individual exposures totaling an effective exposure time of 23 ksec. All of the combined exposures were obtained in photometric conditions or through thin clouds. The data were flux calibrated using observations of Feige 110 (Massey & Gronwall 1990) which provide an effective calibration from 9700–10200Å . Tests with two other standard stars (Feige 34 and Wolf 1346) indicate the relative flux calibration should be much more reliable than the absolute calibration; we have probably suffered from slit losses and possible absorption during the night due to faint cirrus. No emission lines were seen in the extracted NIRSPEC spectra but a faint stellar continuum was detected for both images a and b; the signal is slightly stronger for a.

Although observational selection plays an important role, as most successfully identified $z > 5$ galaxies display intense Lyman α emission (Spinrad 2003), it is interesting to consider the maximum possible *observed* equivalent width, W_{max}, implied by our non-detections in the LRIS and NIRSPEC data. Using our spectrophotometric calibration, assuming a line width of 5Å and a conservative 5σ detection limit, Figure 4 shows W_{max} as a function of wavelength for our data. Although OH airglow emission precludes detection in a few small wavelength regions, for 60% of the important 9000Å–9500Å interval an observed equivalent width larger than 120Å (a value much less than for most high redshift star forming sources, Hu et al 2003) would have been detected. From 9000–9300Å ($6.4 < z < 6.65$) and longward of 9550Å ($z > 6.85$) the constraint is tighter. Because of the much deeper exposures with NIRSPEC and the stronger continuum redward of 9800Å, a more stringent 5σ upper limit of $W_{max} <$60Å is derived for the 9550–11100Å window effectively ruling out any reasonable

level of emission in the redshift range 6.85< z <8.2. Thus it seems reasonable to deduce that, *if the redshift is not in the 6.65< z <6.85 interval*, Lyman α emission is either very weak or absent. It will be important in future, deeper, observations to rule out an emission line hiding in the OH forest at ∼9500Å corresponding to a source at z ∼6.8.

The absence of Lyman α emission in a distant source may seem surprising. However, there are many examples of luminous Lyman break galaxies at lower redshift with weak or no emission (Shapley et al. 2003). Indeed, those authors claim only 20-25% of star-forming examples show Lyman α emission sufficiently prominent to be classified as narrow band excess objects.

The most important outcome of the long NIRSPEC exposure is the detection of a very faint continuum redward of 9800Å (Figure 5). A continuum signal is seen in both images. As it is stronger in image a, we will use this spectrum for the following analysis. Given the absence of Lyman α emission and the inference of a photometric break in the wavelength range 9250–9850Å the key question is therefore the lowest wavelength at which a continuum signal can be seen in the NIRSPEC data.

Inspection of the data reveals a drop in the continuum flux at 9800Å shortward of which there is no reliably detected signal despite a robust photometric calibration (see upper panels of Figure 5). The OH spectrum is fairly clean in this region although there is some atmospheric absorption which could affect the calibration at 9500–9700Å . Although the feature itself is only marginal, the absence of flux below 9800Å seems significant when one considers the photometric data summarised in Figure 3. Specifically, if the UV continuum extended down to 9250Å , as would be the case if the source were at z=6.6, it is difficult to understand why the stellar continuum is not detected to shorter wavelengths (Figure 5). Although this weak feature is the only indicator in our exhaustive attempts to measure a spectroscopic redshift, if it is indeed the cause of the Gunn-Peterson edge inferred from the photometric data, a redshift of z ≃7.05 is implied. In this case, the photometric redshift analysis discussed in S§3.2 would indicate a steep UV continuum slope of α=5.

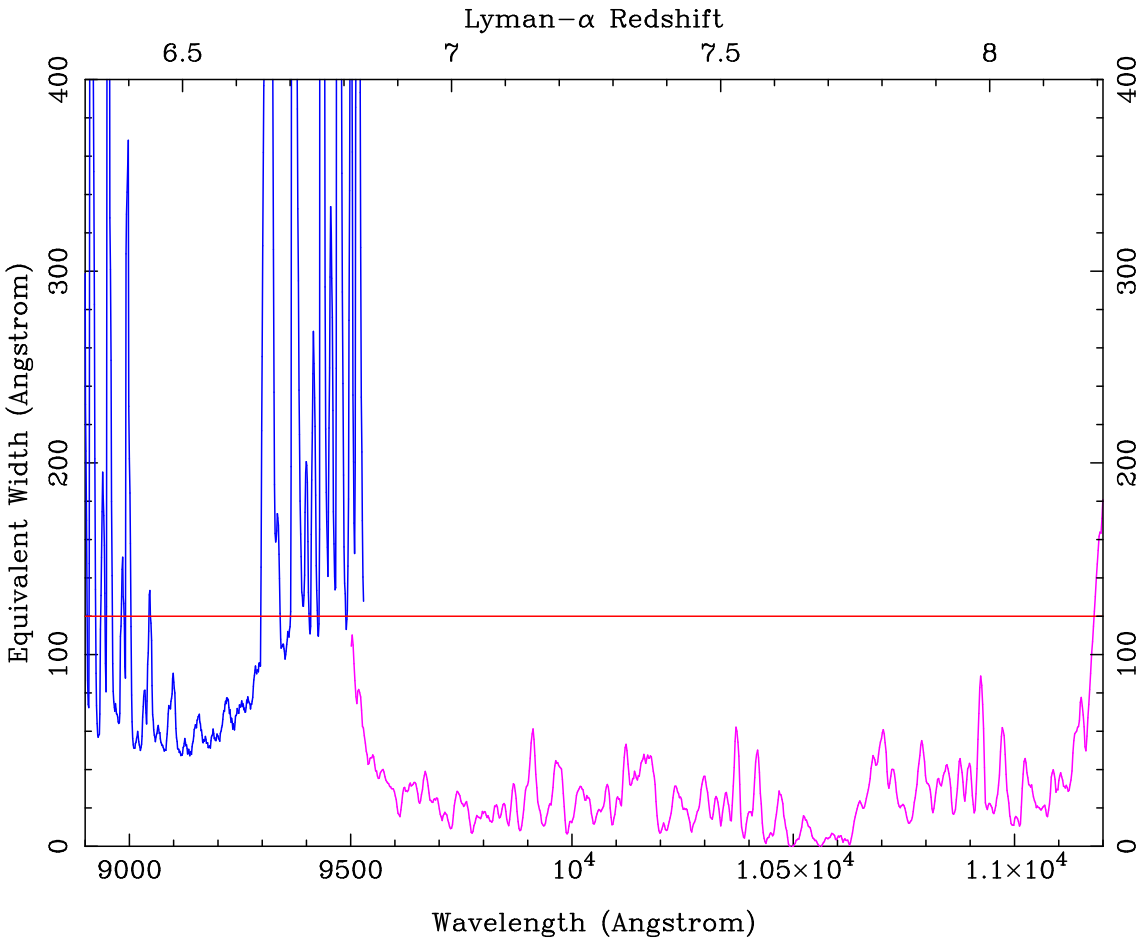

Figure 4 Observed equivalent width detection limit (5σ), W_{max}, for Lyman α emission in the LRIS and NIRSPEC data assuming a line width of 5Å. An emission line stronger than W=120Å(indicated by the horizontal line), corresponding to an integrated line flux of 1.6×10^{-18} ergs s^{-1} cm^{-2}Å^{-1}, would have been seen for 60% of the wavelength range 9000Å–9500Å. Constraints in the range 9000–9300Å and beyond 9550Å are tighter. The longer NIRSPEC integrations provide a maximum equivalent width below W=60Å for the entire 9550–11100Å range, corresponding to an integrated line flux of 7×10^{-19} ergs s^{-1} cm^{-2}Å^{-1}.

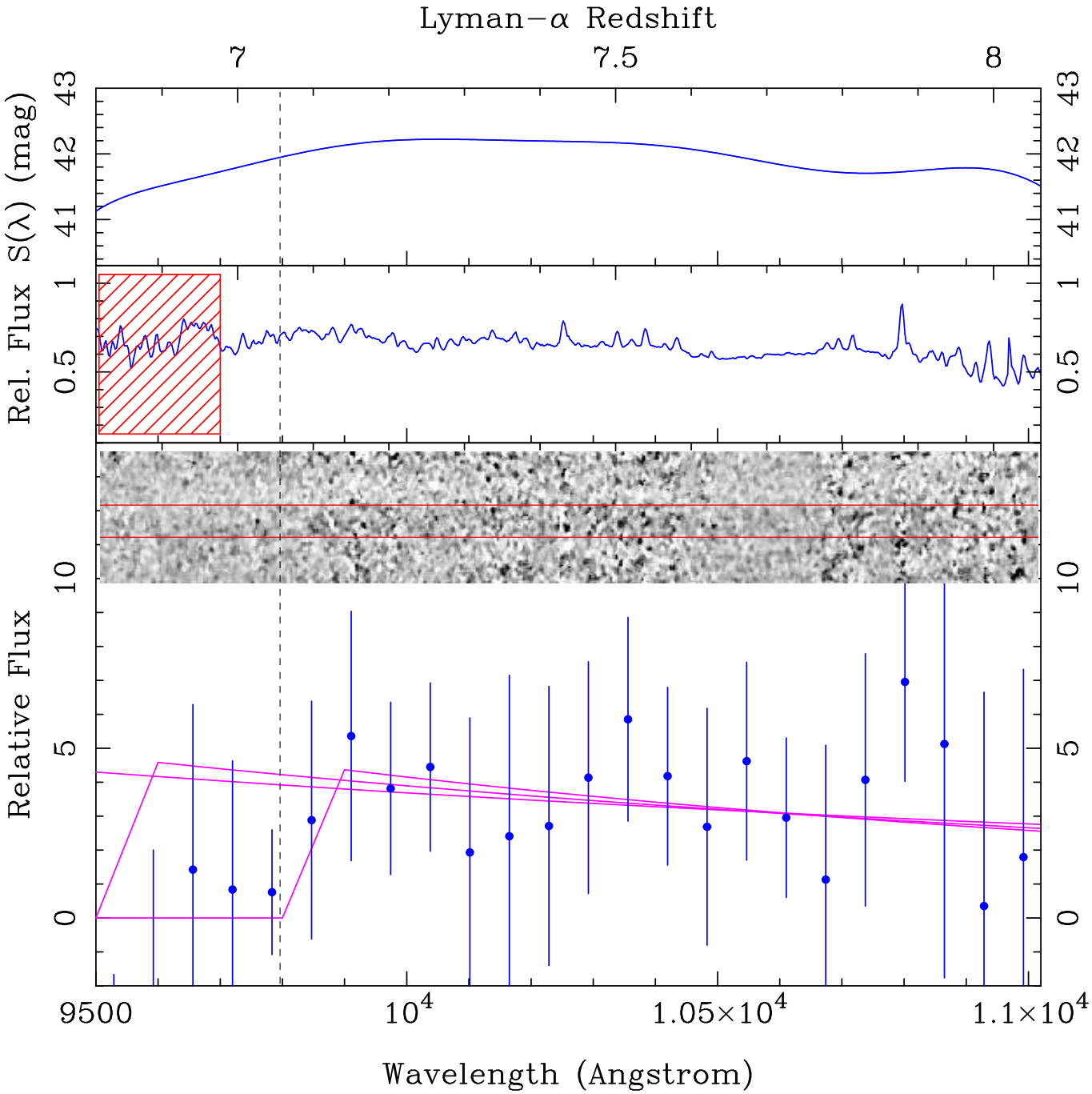

Figure 5 NIRSPEC spectrum for image *a* in the wavelength region 9500Å –1.1μm. (Top) Relative sensitivity of NIRSPEC in the configuration used derived from 3 independent flux calibration stars. Adequate sensitivity is available over the entire range. (Middle) observed spectrum of one of these standards, Feige 110 illustrating *a priori* the absence of any strong atmospheric features in the reduction. The red hashed rectangle indicates the region where variable atmospheric absorption is expected (Massey & Gronwall 1990). (Bottom) Flux calibrated binned spectrum for image *a*. Error bars include the effect of wavelength-dependent OH emission. Curves represent UV SEDs consistent with the photometry (Figure 3) spanning the range 6.6< z <7.1. The absence of significant flux below 9800 Å suggests a redshift at the upper end of this range, i.e. $z \simeq 7$.

5. A z≃7 Source

Clearly identifying the redshift of this source has been extremely challenging and further studies would be highly desirable to confirm our conclusions. We have introduced three independent arguments which, taken in combination, justify why the newly-located multiple images arise via a single lensed source at a redshift $z \sim 7$. First, the geometrical configuration of images a, b and c with respect to the critical line in this well-modeled cluster indicates $z > 6$. We argued that the location of the critical line in the vicinity of the pair is tightly constrained from the successful identification of the earlier source at z=5.576 (Ellis et al 2001). Secondly, there is a strong break indicated in the spectral energy distribution (SED) delineated by the broad-band photometry extending from the F606W to F160W (H) filters, arguing for a redshift $6.6 < z < 7.1$. The lower redshift limit $z > 6.6$ is particularly firm and supported by the absence of any LRIS continuum signal in the wavelength range 9000-9300 Å. Finally the absence of any detectable signal below 9800Å seen in the NIRSPEC continuum argues the redshift lies in the upper end of the photometric range, $z \simeq 7$, as otherwise the rising UV continuum would have been detected.

Even if one disregards the weak feature in the NIRSPEC spectrum, the $6.6 < z < 7.1$ source is of considerable interest since, as we discussed in §3-4, it is difficult to reconcile a spectral break at $\lambda > 9250$Å with a UV continuum slope of $\alpha \lesssim 3$, assuming the UV continuum is described by a power law above the Lyman α discontinuity (Figure 3). Starburst models assuming Population II metallicity and a Salpeter stellar initial mass function (IMF) typically produce slopes of $\alpha \lesssim 2$ (Leitherer et al. 1999). Clearly the inferred UV continuum of the $z \sim 7$ source rises faster to shorter wavelengths than for any of the models calibrated with local data. Models based on massive metal-free stars, such as those which may be expected close to the epoch of reionization (Abel, Bryan, & Norman 2000; Bromm, Coppi, & Larson 1999), do produce somewhat steeper UV slopes, $\alpha \simeq 3$ (Schaerer 2002). More precise photometry for this object, particularly in the 1–1.5μm range is needed to understand this issue. If a steep UV slope ($\alpha \geq 3$) is indeed confirmed, the source may represent a promising candidate for a Population III starburst.

The star-formation rate (SFR) of the source can be estimated from the stellar UV continuum luminosity. The unlensed F160W magnitude, $H_{160W} = 26.5 \pm 0.1$, translates into a specific flux of 2.35×10^{-31}erg s^{-1}cm^{-2}Hz^{-1} at 1.6μm, assuming a smooth SED. The intrinsic specific luminosity at 2000Å is then 1.85×10^{28}erg s^{-1} Hz^{-1} implying a SFR of 2.6 M$_\odot$yr^{-1} using Kennicutt's (1998) empirical calibration. We estimate a 15% error arising from uncertainties in the photometry and magnification. This derived SFR is significantly higher than that for the $\simeq 0.5\ M_\odot$ yr^{-1} computed for the lensed source at z=5.576 (Ellis et al. 2001) but within the range of typical Lyman-α emitters at $z \simeq$5.5-6.5.

Our estimated SFR may suffer from two systematic errors. If dust is present, it will dim the UV continuum, causing us to underestimate the value. However, assuming a familiar selective extinction curve, reddening would then imply the intrinsic UV continuum slope is even steeper than $\alpha \simeq$3-5. A second uncertainty arises from our assumed stellar initial mass function (IMF) and metallicity via Kennicutt's local calibration. If the IMF is top-heavy or the metallicity is lower than in local starbursts, the SFR will likely have been over-estimated.

Given the intense star formation, the apparent lack of Lyman α emission is puzzling if dust extinction is not important. Weak or absent Lyman α emission seen in the younger (<1 Gyr) Lyman break galaxies at $z \simeq$3 has been interpreted via the presence of dust shrouds which are eventually disrupted via feedback processes as the stellar population matures (Shapley et al. 2003). As our source is likely younger than 500 Myr, a very specific dust/gas geometry would be needed to strongly extinct the Lyman α photons without reddening the UV continuum. This problem may be exacerbated if the IMF is top-heavy or the metallicity low, since the ionizing photon production rate will be higher making any emission line yet more prominent (c.f. Malhotra & Rhoads 2002).

An alternative explanation for the absence of Lyman α emission may be incomplete reionization at $z \simeq$7. Neutral hydrogen can scatter Lyman α photons after they have escaped the ISM of the emitting galaxy (e.g., Miralda-Escude & Rees 1998). If the source were embedded in a neutral zone, even a strong Lyman α emission line emitted from the galaxy could be quenched. However, in such cases, simulations suggest that emission can still be observed even from sources embedded in fully neutral zones, depending on details of the many relevant parameters of the source (Haiman 2002, Santos 2003).

Since the universe is only 750 Myr old at $z = 7$, the total stellar mass is unlikely to exceed $1 - 2 \times 10^9$ $M_\odot$. Halos of mass $> 1.2 \times 10^{10} M_\odot$ at $z \simeq$7 are quite consistent with conventional structure formation models (Barkana & Loeb 2002) and sufficient to supply baryons to sustain the observed star formation rate. The instantaneous baryonic accretion rate for such a halo at $z = 7$ is, on average, 4.4 $M_\odot yr^{-1}$ (e.g. Lacey & Cole 1993), so even if an earlier starburst consumed most of the baryons, they can be rapidly replenished. Although we have no constraints on the actual star-formation history, these arguments emphasize that we are not necessarily viewing the system at a special time in its evolution.

The strong magnification ($\simeq \times$25) of the two brighter images gives us our first glimpse into the morphological structure of a very distant source on sub-kpc scales. Both images a and b have a bright core, a second fainter knot, and extended emission of lower surface brightness (Figure 1). There is no noticeable color gradient. Our mass model for Abell 2218 implies magnifications of $\sim \times$15 along the major axis of images a and b, and $\sim \times$1.7 along the minor axis. The 0.15″ width of the F850LP PSF translates into a physical resolution of

$\sim$470 pc along the minor axis and $\sim$50 pc along the major axis.

We thus infer that the source (observed with $3.6'' \times < 0.15''$) has a maximum physical size of 1.2 kpc by <500 pc. The maximal associated area of 0.6 kpc^2 indicates a star-formation surface density in excess of 4.3 $M_\odot yr^{-1} kpc^{-2}$. The bright knot is only 100 pc across implying a star-formation surface density in the range $\sim$50-250 $M_\odot yr^{-1} kpc^{-2}$ depending on the exact geometry, comparable to the most intense starburst activity observed locally (Kennicutt 1998).

If this source is typical of those which reionized the Universe in a narrow time interval of $\Delta\, z$=1 around $z \simeq$7, we can estimate the expected surface density from the arguments presented by Stiavelli et al (2003). Depending on the source temperature, Lyman continuum escape fraction and clumpiness of the IGM, we would deduce surface densities $n \simeq$0.3-5 arcmin^{-2} are necessary. In as much as it is possible to estimate the actual surface density from one source and the limited area examined by looking through only one cluster lens to find it, we find a number density of $n \simeq 1 \pm 0.5$ arcmin^{-2}.

In conclusion, we present evidence that we have found a highly magnified source which lies beyond $z \simeq 6.6$, possibly at $z \simeq$7. Even in advance of the infrared capabilities of *JWST*, further observation of this source will be important in determining a more secure redshift, and improving the constraints on the slope of the UV continuum. Further spectroscopy in the 9200Å-1μm region would be valuable to probe any Lyman α emission at $z \simeq$6.8 (Figure 4) and to confirm (or otherwise) the significance of the weak continuum drop seen in the NIRSPEC data at 9800Å . The location of the Gunn-Peterson trough might also be verified more precisely via narrow band imaging through gaps in OH forest and with a deep ACS grism spectroscopy.

Notwithstanding the need for further work and regardless of its precise redshift in the constrained window 6.6< z <7.1, our source appears to be a star-forming galaxy with intriguing spectral properties, possibly representative of a new population responsible for ending cosmic reionization. While our discovery highlights many of the challenges facing searches for those z >6.5 galaxies responsible for reionization, it also demonstrates the ability of strong lensing by clusters of galaxies to locate and reveal the detailed properties of high redshift sources. The lensed galaxy presented in this paper, if observed unlensed at $z_{AB} \sim 28.5$ would lie at the detection limit of the upcoming UDF observation[7] and no spectroscopic follow-up would have been possible.

[7]http://www.stsci.edu/hst/udf/parameters

We thank Fred Chaffee for his continued encouragement to track down the nature of this intriguing system and acknowledge useful discussions with Bob Abraham, Chris Conselice, Graham Smith, Mark Sullivan and Tommaso Treu. Hy Spinrad and Andy Bunker are thanked for reading an earlier version of this manuscript and offering valuable suggestions. We thank two anonymous referees for their valuable comments which significantly improved the presentation of our data. Alice Shapley and Dawn Erb for helpful advice on the optimum procedures for obtaining and reducing faint NIRSPEC data. We also thank James Larkin and James Graham for their advice concerning the use of NIRSPEC in the 1μm wavelength region. Andrew Blain and Naveen Reddy kindly provided access to the Keck NIRC observations. Faint object spectroscopy at the Keck observatory is made possible through the dedicated efforts of Ian McLean and collaborators for NIRSPEC, and Judy Cohen, Bev Oke, Chuck Steidel and colleagues at Caltech for LRIS. JPK acknowledges support from Caltech and CNRS. MRS acknowledges the support of NASA GSRP grant NGT5-50339. The study of Abell 2218 as a cosmic lens is supported by NASA STScI grant HST-GO-09452.01-A.

REFERENCES

Abel, T., Bryan, G. L., & Norman, M. L. 2000, *Astrophys. J.*, **540**, 39

Barkana, R., Loeb, A., 2002, *Astrophys. J.*, **578**, 1.

Becker, R. H. et al. (SDSS Collaboration) 2001, *Astron. J.*, **122**, 2850.

Bouwens, R. J. et al, 2001, *Astrophys. J.*, **595**, 589.

Bromm, V., Coppi, P. S., & Larson, R. B. 1999, *Astrophys. J. Lett*, **527**, L5

Dickinson, M. et al, 2003, *Astrophys. J. Lett* sumitted (astro-ph/0309070)

Djorgovski, S.G., Castro, S.M., Stern, D. & Mahabal, A.A. 2001, *Astrophys. J. Lett*, **560**, L5.

Ebbels, T., Ellis, R.S., Kneib, J-P., Leborgne, J-F., Pellò, R., Smail, I.R. & Sanahuja, B. 1999, *Mon. Not. R. astr. Soc.*, **295**, 75.

Ellis, R.S., Santos, M.R., Kneib, J-P, Kuijken, K., 2001, *Astrophys. J. Lett*, **560**, L119.

Fan, X. et al. (SDSS Collaboration) 2002, *Astron. J.*, **123**, 1247.

Haiman, Z. 2002, *Astrophys. J. Lett*, **576**, L1

Hu, E.M., Cowie, L.L. & McMahon, R.G. 1998, *Astrophys. J.*, **502**, L99.

Hu, E.M., Cowie, L.L., Capak, P., McMahon, R.G., Hayashimo, T., Komiyama Y., 2004, to appear in *Astron. J.* (astro-ph/0311528)

Kennicutt, R.C. 1998, *Ann. Rev. Astron. Astr.*, **36**, 189.

Kneib, J.-P, Ellis, R.S., Smail, I.R., Couch, W.J. & Sharples, R.M. 1996, *Astrophys. J.*, **471**, 643.

Kneib, J.-P., van der Werf, P., Kraiberg, K., Smail, I., Blain, A., Frayer, D., Barnard, V., Ivison, R., 2004a, *Mon. Not. R. astr. Soc.*, in press.

Kneib, J.-P. et al, 2004b, in preparation.

Kodaira, K. et al. 2003, *P.A.S.J. Lett*, **55**, L17.

Kogut, A. et al. 2003, *Astrophys. J. Suppl.*, **148**, 161.

Lacey, C. & Cole, S. 1993, *Mon. Not. R. astr. Soc.*, **262**, 627

Leitherer, C., Schaerer, D., Goldader, J.D. 1999, *Astrophys. J. Suppl.*, **123**, 3.

Malhotra, S. et al. 2001, in *Gas and Galaxy Evolution*, eds. Hibbard, J.E. et al, ASP Conf. Series (astro-ph/0102140)

Malhotra, S. & Rhoads, J. E. 2002, *Astrophys. J. Lett*, **565**, L71

Massey, P. & Gronwall, C. 1990, *Astrophys. J.*, **358**, 344

McLean, I. S. et al. 1998, Proc. SPIE, **3354**, 566

Miralda-Escude, J. & Rees, M. J. 1998,*Astrophys. J.*, **497**, 21

Oke, J.B. et al. 1995, *Publ. Astr. Soc. Pac.*, **107**, 375.

Santos, M.R., 2003, *Mon. Not. R. astr. Soc.*, sumitted astro-ph/0308196

Santos, M.R., Ellis, R.S., Kneib, J-P, Richard, J., Kuijken, K., 2003, *Astrophys. J.* sumitted (astro-ph/0310478)

Schaerer, D., 2002, *Astronomy & Astrophysics*, **382**, 28.

Shapley, A.E., Steidel, C.C., Pettini, M., Adelberger, K.L., 2003, *Astrophys. J.*, **588**, 65.

Spergel, D.N. et al. 2003, *Astrophys. J. Suppl.*, **148**, 175.

Spinrad, H., 2003, in *Astrophysics Update*, Mason J. (Ed.) (astro-ph/0308411)

Spinrad, H., Stern, D., Bunker, A., Dey, A., Lanzetta, K., Yahil, A., Pascarelle, S., Fernandez-Soto, A. 2003, *Astron. J*, **116**, 2617.

Stanway, E., Bunker, A., Mc Mahon, R., Ellis, R.S., Treu, T., Mc Carthy, P., 2003, *Astrophys. J.* sumitted (astro-ph/0308124)

Stern, D. & Spinrad, H. 1999, *Publ. Astron. Soc. Pac.*, **111**, 1475.

Stiavelli, M., Fall, S.M., Panagia, N. 2004, *Astrophys. J.*, in press.

Weymann, R. J., Stern, D., Bunker, A., Spinrad, H., Chaffee, F. H., Thompson, R. I., & Storrie-Lombardi, L. J. 1998, *Astrophys. J. Lett*, **505**, L95

Yan, H., Windhorst, R.A., Cohen, S.H., 2003, *Astrophys. J. Lett*, **585**, L93.

Table 1. Observed Photometry for the Triple System

	a	b	c
α_{J2000}	16:35:54.73	16:35:54.40	16:35:48.92
δ_{J2000}	66:12:39.00	66:12:32.80	66:12:02.45
V_{606W}	not detected	not detected	not detected
I_{814W}	26.5±0.2	26.4±0.2	not detected
z_{850LP}	24.38±0.05	24.54±0.05	25.9±0.1
J	23.4±0.3	23.5±0.3	—
H_{160W}	22.96±0.06	23.01±0.07	—
V_{606W}-z_{850LP}	>3.6	>3.5	>2.1
I_{814W}-z_{850LP}	2.1±0.2	1.9±0.2	>1.8
z_{850LP}-J	1.0±0.3	1.0±0.4	—
z_{850LP}-H_{160W}	1.42±0.1	1.53±0.1	—
Magnification	25±3	25±3	5.3±0.5

3σ detection limits for a point source:
$V_{606W} = 28.0$, $I_{814W} = 27.2$, $z_{850LP} = 26.7$, $J = 24.4$, $H_{160W} = 25.8$.

This figure "f2.jpg" is available in "jpg" format from:

http://lanl.arXiv.org/ps/astro-ph/0402319